The photoelectron spectra of the isomeric 1- and 2-methyltetrazoles; their equilibrium structures and vibrational analysis by ab *initio* calculations.

Michael H. Palmer,[1,a] Marcello Coreno,[2,b] Monica de Simone,[3,b] Cesare Grazioli,[2] Søren Vrønning Hoffmann,[4,b] Nykola C. Jones,[4,b] Kirk A. Peterson,[5,b] R. Alan Aitken[6] and Cécile Rouxel.[6]

[1] *School of Chemistry, University of Edinburgh, Joseph Black Building, David Brewster Road, Edinburgh EH9 3FJ, Scotland, UK*

[2] ISM-CNR, Istituto di Struttura della Materia, LD2 Unit 34149 Trieste, Italy

[3] *IOM-CNR Laboratorio TASC, Trieste, Italy*

[4] *ISA, Department of Physics and Astronomy, Aarhus University, Ny Munkegade 120, DK-8000 Aarhus C, Denmark*

[5] *Washington State University, Department of Chemistry, Pullman, WA 99164-4630, USA*

[6] *School of Chemistry, University of St Andrews, North Haugh, St Andrews, Fife, KY16 9ST, U. K.*

[a)] Email: *m.h.palmer@ed.ac.uk*: Telephone: +44 (0) 131 650 4765

[b)] Electronic addresses: *malgorzata.biczysko@sns.it; marcello.coreno@elettra.eu; desimone@iom.cnr.it; vronning@phys.au.dk; nykj@phys.au.dk; kipeters@wsu.edu; grazioli@ism.cnr.it; raa@st-and.ac.uk*

ABSTRACT

New synchrotron based studies of the photoelectron ionization spectra (PES) for the isomeric 1- and 2-methyltetrazoles (***1-*** and ***2-MeTet***) show markedly higher resolution than previous reports. The unusual spectral profiles suggest that considerable overlay of the ionic states occurs for both molecules. Under these circumstances of near degeneracy of two or more ionic states, mutual annihilation of vibrational fine structure occurs, for all except the strongest vibrational states; the PES just reflects the resultants rather than full spectra. Theoretical determination of the adiabatic ionization energies (AIE) proved a challenge; the most successful method was second order Møller-Plesset perturbation theory (MP2). These calculations suggest that the lowest PES bands for both isomers, contain ionization both from lone pair σ-orbitals ($^2A'$) on the N-atoms (LP_N) and π-orbitals ($^2A''$). The lowest experimental

AIE are: ***1-MeTet,*** 10.315 eV assigned to $1^2A^{/}$, while ***2-MeTe***t, is 10.543 eV assigned to $1^2A^{//}$. Franck-Condon (FC) analysis shows that the lowest ionization energy regions of both spectra are dominated by IE from the $LP_N\ ^2A^{/}$ manifold, even though the $^2A^{//}$ states have higher absolute intensity. In this example, we have utilization of a VUV Rydberg state to assist simplification of the PES; more frequently, the PES assignment is simpler, and assists the location of Rydberg states in the VUV. The very slow spectral onset for ***2-MeTet*** demonstrates the importance of vertical ionization energy (VIE) calculations, since maxima are more readily measured than slow onsets. These were performed at the equilibrium structure of the $X^1A^{/}$ state, using both multi-reference multi-root configuration interaction (MRD-CI), and the ionization potential (IP) variant of the equations-of-motion coupled cluster method, with single and double excitations (EOMIP-CCSD). This enabled the principal ionization bands to be identified over a wider range of energy.

Attempts to study the higher ionic states by EOMIP-CCSD, showed several states of each symmetry are close to degenerate for ***1-MeTet*** in particular. A multi-configuration self-consistent field (MCSCF) study confirmed the small separation of ionic states, but state switching during the optimization process largely disabled this method.

INTRODUCTION

The azoles are fully conjugated, potentially aromatic, ring systems which contain one or more N-atoms in a 5-membered carbocyclic ring. Azoles occur widely in nature, where diverse examples include biotin (vitamin B_7) and nicotine. The pharmacological activity of numerous azoles,[1] has led to major academic and industrial research. Important synthetic products are exemplified by fluconazole (a potent antifungal triazole), and candesartan (an antihypertensive tetrazole). We have previously reported combined PES and VUV spectral studies for several azoles, such as the 1, 2, 3- and 1, 2, 4-triazoles,[2,3] where three C-H units in the 5-membered ring are replaced by N-atoms. We now extend this study to the 1,2,3,4-tetrazole ring system,

where only one C-atom remains in the ring.[4] It has been used in automobile airbags, owing to its facile release of nitrogen gas.[4] Although pentazole derivatives, with 5 N atoms in a ring are known, so far they have exhibited limited interest or utility.

Tetrazole is a mixture of two tautomers, ***1*** and ***2*** (***R = H***), shown in Fig. 1; these interconvert in gaseous or solution phases, but NMR spectra of the individual forms have been observed in suitable solvents.[5,6] The ***N-CH₃*** compounds in Fig.1 where ***R = Me***, do not interconvert. We have prepared these to perform an unambiguous study of the individual ring systems ***1*** and ***2***. For simplicity, ***1*** and ***2*** (***R = Me***) in Fig. 1, are abbreviated to ***1-MeTet*** and ***2-MeTet***. Both molecules have three classical lone pairs on the ***N***-atoms (LP_N); the conformations shown in Fig.2 are the most stable for the neutral molecule.

HeI irradiation PES (21.22 eV) of ***1*** and ***2*** (***R = H***) showed the close relationship of tetrazole to the other azoles. CI calculations led to the proposal that mixing of LP_N will occur when several are present.[7] The dominance of the ***2H***-tautomer of tetrazole in the gas phase was later established using HeII radiation (He^{++}, 40.82 eV);[8] this minor component in the HeI beam (HeI_α, 21.22 eV),[8] showed that comparison of the PES spectral profiles of tetrazole itself with those of ***1-MeTet*** and ***2-MeTet*** (Fig. 1, ***R = Me***) was unambiguous.[8] Later, configuration interaction (CI) studies supported this conclusion.[9] We now report a synchrotron based high-resolution PES, in Fig.3, which shows significant fine structure. The experimental study is accompanied by a detailed theoretical analysis using high-level ab initio studies, following our recent work on mono-halogenobenzenes (***C_6H_5X***, where ***X = F, Cl, Br*** and ***I***) and ***CH_2F_2***.[10,11]

II. EXPERIMENTAL AND COMPUTATIONAL PROCEDURES

(a) **Synthesis.** The structurally secure synthesis of both ***1-*** and ***2-MeTet,*** and their spectral identification by nuclear magnetic resonance (NMR) are described in the supplementary material as SM1.

(b) Photoelectron spectral studies of *1-MeTet* and *2-MeTet.* These were obtained at the Gas Phase Photoemission beam line of the Elettra synchrotron, as described previously.[10,11] ***1-MeTet*** vapour was expanded under vacuum close to its melting point. The higher vapour pressure of ***2-MeTet*** enabled use of a simple gas line at room temperature. The irradiation energy for the main study was 30 eV; this leads to an overall energy resolution of 11 meV (89 cm^{-1}). The spectral range from 7.767 to 15.578 eV contains 7992 data points with a spacing of 1 meV. A wider energy range from 7.767 to 39.937 eV was recorded using a beam energy of 95 eV; this had overall resolution better than 30 meV, while the 3400 data points had a spacing of 10 meV. Comparison of the two PES spectra for the low ionization energy range are shown in Fig. 3. The wide scans are shown in the supplementary material as SM2. Throughout this paper, PES and electronic origins are described in electron volt (eV) units; all vibration frequencies are in units of cm^{-1}.

(c) Theoretical methods for AIE. The calculated sequence by symmetry of the theoretical adiabatic ionization energy (AIE) proved difficult to determine. The principal results described here used second order Moller-Plesset (MP2) perturbation theory in GAUSSIAN-09 (*G-09*) [12] and GAMESS-UK.[13] An important aspect using GAMESS-UK is the particular implementation of 'level shifting' in order to obtain convergence in self-consistent field (SCF) calculations. The level shifting,[14,15] written for the ATMOL suite, allows interactions between the doubly occupied and partially occupied MOs, and the occupied with virtual orbital interactions to be treated separately. This assists both SCF and MP2 calculations of higher ionic states to be obtained; normally, without this level shifting procedure, attempts by switching the singly occupied MO would lead to the higher energy state collapsing to the lowest energy state. Here we found that two highest states of each symmetry were evaluated with the ***1-MeTet*** system. Unfortunately, with ***2-MeTet*** we were only able to obtain the first root of each symmetry.

(d) More sophisticated theoretical procedures. Initially we used two more advanced procedures. These were equations-of-motion coupled cluster calculations, including single and double excitations (EOM-CCSD), with the related ionization potential (energy) code EOMIP-CCSD[16-18] in the CFOUR suite,[19] and multi-configuration self-consistent field (MCSCF) in MOLPRO.[20] In both these methods, the lowest state of each symmetry proceeded normally. However, attempts to select higher roots led to state switching during structural optimization. Very small energy separations occur between ionic states of either symmetry ($^2A'$ or $^2A''$) for both ***1-MeTet*** and ***2-MeTet***. The potential energy surface interactions for the $1^2A''$ and $2^2A''$ states occur for all sets of structural parameters used, with similar effects in the $^2A'$ series. Although this limited the use of these methods here, the principal results for all procedures, including the MP2 ones, are shown in Table I.

(e) Vertical ionization energies (VIE) studies. We used the multi-reference multi-root configuration interaction (MRD-CI) code[21] in GAMESS-UK, as well as EOMIP-CCSD to calculate VIE. The sequence of ionic states are determined at the X^1A' equilibrium structure, so that potential energy surface issues cannot occur.

(f) Basis sets. The augmented-correlation consistent triple zeta valence with polarisation (aug-cc-pVTZ) basis sets were used for both MP2 and EOMIP-CCSD calculations.[22] The Ahlrichs Group default series 2, triple zeta valence with polarisation (def2-TZVP) basis sets[23,24] were used in *G-09* and MOLPRO.

(g) Franck-Condon (FC) analyses. The MP2 results using the *G-09*[12] suite, allow direct analysis of the harmonic frequencies by the Pisa software.[25-29]

III. RESULTS

A. Initial comments. The ***CH_3*** groups in both ***1-MeTet*** and ***2-MeTet*** show internal rotation barriers. Exploratory computations for both compounds, using MP2 and Restricted-Hartree-Fock (RHF) methods, showed that these barriers are negligible in relation to the

ionization processes. These are shown in the supplementary material under SM3. The lowest energy rotational states show only positive harmonic vibrational frequencies. Consideration of C_1 symmetry conformers proved unnecessary, and enabled the sigma/pi separation in C_S symmetry to be generally applied here. There is a crystallographic study of ***1-MeTet***,[30] but no experimental structure for the ***2-MeTet*** system. The ground and ionic state structures are not central to the present study, and are detailed in the supplementary material as SM4 and SM4.1 respectively.

The highest occupied group of 4 MOs for ***1-MeTet*** is shown in Fig. 4; two of these ($17a^{/}$ and $18a^{/}$) confirm the molecular orbital (MO) interaction between the LP_N, predicted in our previous studies.[7,8,9] The corresponding highest occupied group of 4 MOs for the ***2-MeTet*** series is shown in the supplementary material under SM5.

B. The calculated ionic state sequences for *1-* and *2-MeTet* by AIE and VIE methods.

All conjugated 5-membered ring heterocycles including ***1-*** and ***2-MeTet***, have a 6π-electron ring system with an additional 2π-electrons from the methyl group antisymmetric MO combination of H-orbitals. The latter occur at higher energy and are largely independent of the 6π set.[7,8,9,31] The 6π-electron system is analogous to benzene,[32,33] but the $A^{//} + E^{//}$ states (with doubly occupied MOs, $a_{2u}^2 + e_{1g}^2$) is perturbed in the azoles, owing to the reduced symmetry. The electron density contours shown in Fig.4 demonstrate this for the two highest π-MOs, while the two LP_N MOs shown demonstrate mixing of the LP_N centers in the σ-system.

The ionic state sequence for tetrazole (Fig.1, ***R=H***) by extensive CI at the equilibrium structures,[9] has shown that ***2H***-tetrazole is energetically favorable over the ***1H***-tautomer. We agree with this assignment for the parent compound.

Both the EOMIP-CCSD and MRD-CI calculations shown in Table I, indicate 4 VIE lie under the PES in the 10 to 12 eV region. The calculated ionic state sequences by symmetry are very similar. Indeed, the two sets of calculated energies show a linear relationship for the data in

Table I, with adjacent R^2 correlation coefficient 0.993, but with a slope of 0.839; this slope is an indication of the higher level of configuration interaction in the MRD-CI results. These two sets of calculated ionic state energies are effectively interchangeable. The experimental PES band areas for both compounds, show two peaks and suggest that these occur in a 2: 2 ratio. The VIE results show a sequence of states by symmetry for ***2-MeTet*** as: $1^2A'' < 1^2A' < 2^2A'' < 2^2A'$; alternatively expressed as: $4\pi^{-1} < LP_N^{-1} < 3\pi^{-1} < LP_N^{-1}$. The spacing is consistent with the experimental 2: 2 ratio for this isomer. For ***1-MeTet***, the ionic state sequence is very different: $1^2A' < 2^2A' < 1^2A'' < 2^2A''$. Expressed in terms of electron loss from individual MOs these are: $LP_N^{-1} < LP_N^{-1} < 4\pi^{-1} < 3\pi^{-1}$. However, the last three states are separated in energy by only 0.06 eV (EOMIP) or 0.21 eV (MRD-CI). The overall group is closer to 1: 3 in ratio which makes the AIE results disappointing for the ***1-***isomer.

The theoretical assignment for the PES onset of both isomers strongly suggests that the AIE for ***2-MeTet*** is $1^2A'' < 1^2A'$, but reversed for ***1-MeTet*** to $1^2A' < 1^2A''$. This conclusion is supported by most methods shown in Table I.

Overall, MP2 results in Table I, using the aug-cc-pVTZ basis set functions, gave the most acceptable results for the AIE; the results for the PES analyses below use these values.

C. Vibrational analysis of the ground and ionic states of *1-* and *2-MeTet.*

The vibrational modes for both molecules under C_S symmetry are $1a'$ to $16a'$, and $17a''$ to $24a''$, and are shown in Table II. Single imaginary frequencies were obtained for 2 ionic states, are a'' non-symmetric modes, which have little effect in the Franck-Condon analyses. The imaginary modes result from structural saddle points rather than true minima, but are an insufficient reason to reduce the symmetry to C_1.

D. Franck-Condon analysis of the 10 to 12 eV region of the experimental photoelectron spectrum for *1-MeTet*.

The experimental onset at 10.315 eV (83197 cm^{-1}) has a narrow peak; the linewidth, defined as Full-Width at Half-Maximum (FWHM) is 71 cm^{-1}. This is close to that for an isolated PES

peak where our previous studies[10,11] indicate a FWHM close to 75 cm^{-1}. The two lowest calculated AIE for ***1-MeTet*** are both LP_N ionizations ($1^2A'$ and $2^2A'$). These have small energy separations of 659 cm^{-1} (UHF-MP2) or 2758 cm^{-1} (EOMIP-CCSD). The lowest $1^2A''$ state is calculated to lie 0.982 eV (7920 cm^{-1}) higher in energy. However, there is a major difference in intensities for these two states, with the X^2A' state vibrations generally much weaker. Direct processing of the UHF-MP2 data for the lowest ionic state X^2A' gives the principal FC vibrational contributors to the state shown in Table III. The relative intensities of the theoretical 0-0 transitions for the two states indicate that the $^2A'$ state is responsible for the PES onset. A comparison of the theoretical and experimental PES in Fig. 5, shows that most of the low energy PES structure is reproduced by the $^2A'$ calculation. The higher intensity vibrations of the $^2A''$ state have a 'best fit' onset near 10.613 eV (86000 cm^{-1}), as discussed below. The most intense contributions to the vibrational envelope for the $^2A'$ state are from the a_1 modes 4, 8, 10, 12 and 13. The first three major PES peaks for ***1-MeTet*** have a measured separation of 1323 cm^{-1}. These peak separations are dominated by the 8^1 and 8^2 vibrations of the X^2A' state (Table III), but are the resultants of several contributing vibrations rather than a single vibration. More detailed investigation of the experimental onset for ***1-MeTet*** by double differentiation of the PES band, shows that it contains several unevenly spaced shoulders; the separations range from 51 cm^{-1} on the low ionization side, to 34 cm^{-1} on the higher IE side, and probably reflect part of the hot band profile.

The 0-0 band of the A^2A'' state is not well defined in the PES, but the theoretical profile of this state shows a very strong 0-0 band. Direct comparison with the PES region above 86000 cm^{-1} shows that this state can best be accommodated as shown in Fig. 6. The agreement between the FC profile and PES experiment is much improved when the FWHM for this state is increased, as we have discussed previously.[10,11]

In a later study of the VUV spectra of these two compounds, we will show that two Rydberg states observed near 7.166 eV of the VUV spectrum of ***1-MeTet*** only exhibit the first 2 out of the 3 PES peaks shown in Fig. 5. A more detailed example for ***2-MeTet*** is shown below.

E. Franck-Condon analysis of the 10 to 12 eV region of the experimental photoelectron spectrum for *2-MeTet*.

The very slow onset to the experimental PES for ***2-MeTet***, shown in Figs. 3 and 7 is unusual, and contains a series of relatively sharp peaks superimposed on a broad rising background. The only well-defined features in the PES onset region are AIE at 10.545 eV (85058 cm^{-1}) and a higher feature at 13.197 eV. The apparent VIE at 10.793 eV is probably the result of sharp peaks being superimposed on a broad featureless maximum.

The calculated energy range from 10.18 eV to 11.40 eV (82000 to 92000 cm^{-1}) contains two ionic states. These are $X^2A^{/}$ and $A^2A^{//}$ with a small energy separation of only 0.174 eV (1401 cm^{-1}). Overlay of their vibrational profiles is inevitable, and this near degeneracy is expected to degrade the vibrational structure of both states, as discussed below.

The PES shows doublets near 86000 and 88000 cm^{-1}, and since neither of the calculated FC profiles for these ionic states show intense closely spaced ('split') peaks, we conclude the pairs of peaks arise from one vibration for each of two states. Two of the PES peaks, separated by 0.137 eV (1102 cm^{-1}), are narrower than the others; the lower at 85085 cm^{-1} is attributed to the 0-0 band of the $^2A^{//}$ state, since this calculated state has a high 0-0 band with rapid diminution of its vibrational tail. The only plausible positions for these two theoretical ***2-MeTet*** FC profiles are shown in Fig. 7 in red and blue, with the predicted apparent degeneracy at 10.538 eV. The onset of the $^2A^{/}$ state is not visible, but after super-position of the two profiles onto the observed PES, we assign the 0-0 band of the weak onset state to near 83000 cm^{-1} (10.290 eV). The principal calculated sequences exhibited in Fig. 7, are shown in Table IV, which contains the principal normal modes and low-lying combination bands with high intensity.

Several fundamental vibrational modes of ***2-MeTet*** have high calculated intensities for these ionic states. For $^2A'$, mode 14 is dominant and also appears in many combination bands. But neither of the two lowest modes 15 and 16 (754 and 403 cm^{-1} respectively) are significant. In contrast, for the $^2A''$ state, all of the modes 12 through 16 make important contributions to the vibrational profile. Many of these also occur with considerable intensity in combination bands. Overall however, the X^2A' is much higher in cross-section than the A^2A'' state, the reverse to that for ***1-MeTet***.

Clearly, not all of the sharp peaks shown in Fig. 7 can be accounted for by a single ionic state. As stated in Section III.D for ***1-MeTet***, Rydberg state analysis in the VUV spectrum for ***2-MeTet*** supports this view. After a linear shift, superposition of the PES spectrum for ***2-MeTet*** near 65000cm^{-1} (8.0 eV) in the VUV is shown in Fig.8. Two weak peaks in the PES superimposed at 7.93 eV and 8.40 eV are absent in the VUV. These peaks in the superimposed PES must arise from a second ionic state.

IV. CONCLUSIONS IN RELATION TO THE *1-MeTet AND 2-MeTet* PES ASSIGNMENTS

For ***1-MeTet,*** the calculated FC vibrational profile superimposed in Fig. 5, accounts for most of the principal PES features. However, analysis in terms of a single vibration with an observed but apparent frequency near 1323 cm^{-1} can be excluded. The major peaks are closely spaced vibrational multiplets, in which many combination bands contribute to the vibrational profile. Those shown in Table III are largely combinations of the normal modes. Similar results occur with the ***2-MeTet***.

Even close to the spectral onsets, the high-resolution PES for ***1-MeTet*** and ***2-MeTet*** exhibit considerable complexity, which leads to unusual spectral profiles. The small separations of the ionizations in the PES is interpreted in terms of overlay of the vibrational patterns. The present theoretical methods suggest that the 10 to 12 eV range for both compounds contains four ionic

states, which occur as two pairs of $^2A^{/} + {}^2A^{//}$ states; however, the symmetry sequences differ between the two compounds. The small separations in energy between states of same symmetry lead to state switching during structural optimization; this limits the achievement of calculations at the MCSCF and EOMIP-CCSD levels. Most calculations of this type use energy as their main criterion for state sequence. The current study has a need for an eigenvector following mode where a particular state eigenvector is followed, irrespective of its energy, during the optimization. The present calculations do not give a satisfactory spacing between the observed ionic states when compared with the PES. Fortunately, progress was made using MP2 optimized structures for both first and second ionic states of each symmetry for ***1-MeTet***. This was facilitated by careful use of 'level shifting' during the optimizations; however, the same process failed with ***2-MeTet***. The calculated spectra superimposed in Figs. 5 to 7 are based on MP2 calculations using the aug-cc-pVTZ basis set.

We have previously shown that when two or more IE occur in close proximity, the vibrational patterns expected, although present on the lower energy state, do not occur on the higher energy state. In effect, interference occurs, and residual vibrational structure on the higher state can only be interpreted by major increase in the line width used for the individual vibrations. This line width, described in terms of FWHM, is close to 75 cm^{-1} for isolated vibrations, but has to be increased to 400 cm^{-1} or more in the more extreme cases. The overlay of ionic states, exposed in our previous studies of other systems, occurs in a major way here, and produces serious problems for comparison with theoretical envelopes. The PES becomes a skeleton of the strongest vibrations superimposed on a multitude of weak peaks which become a semi-continuum.

Line broadening has become a feature of our investigations of the FC structure in high-resolution PES when two or more AIE are close, or even overlay.[10,11] As in our previous studies,[10,11] this effect appeared to be unidirectional, since the effect on the lower IE seems

relatively small, while much of the structure of the higher IE is destroyed. In the present case, we believe that the PES of ***2-MeTet*** in particular, merely shows the remnants of a mutual destruction of the weaker vibrational state, owing to the near degeneracy.

In this study, we have utilized a VUV Rydberg state to assist simplification of the PES. The reverse occurs more frequently since the PES assignment is frequently simpler, and assists the location of Rydberg states in the VUV. Differences in the quantum defect between two Rydberg states, having nearly degenerate ionizations in the PES, can lead to VUV Rydberg states which are separate. Joint study of both types of spectra can lead to synergy and assist the interpretation of both; this will remove complications which may occur when the two studies are not performed together.

Most analyses from the early years of photoelectron spectroscopy, attempted to correlate apparent vibrations in PES with those in the neutral ground state.[37,38] The present work, supports our previous conclusions, both for difluoromethane and the halogenobenzenes, that this is simplistic. Apparent 'vibrations' in both the PES and VUV spectra are merely the resultant of super-position of several individual vibrations..

Supplementary Material

The Supplementary Material Contents are as follows:

Contents:

Acknowledgements

We thank: (a) the Elettra Synchrotron facility for a Grant of beamtime; (b) the ASTRID2 facility for grants to carry out the parallel VUV absorption study; (c) the Italian MIUR (under the project PON01-01078/8); (d) the University of Edinburgh EPCC super-computing facility for support; (e) Prof. Malgorzata Biczysko for helpful discussions; (f) C. Puglia (Uppsala University, Sweden) and the Carl Tygger Foundation for making available the VG-Scienta SES-200 photoelectron analyser at the Gas Phase beamline, Elettra, Italy.

References.

1. Pfeffer M, Swedberg K, Granger C, Held P, McMurray J, Michelson E, Olofsson B, Ostergren J, Yusuf S, Pocock S, Lancet. ***362,*** 759–66. (2003).
2. M. H. Palmer, S. Vronning Hoffmann, N. C.; Jones, A. R. Head, D. L. Lichtenberger, J. Chem. Phys., **134**, 084309/1-084309/13 (2011).
3. M. H. Palmer, P. J. Camp, S. Vronning Hoffmann, N. C. Jones, A. R. Head, D. L. Lichtenberger, J. Chem. Phys., **136**, 094310/1-094310/11 (2012).
4. R. C. Storr, Science of Synthesis: Houben-Weyl Methods of Molecular Transformations, **13**, 917-922 (2004).
5. D. S. Wofford, D. M. Forkey, J. G. Russell, J. Org. Chem., **47**, 5132 (1982).
6. N. N.Sveshnikov, J. H. Nelson, Magnetic Resonance in Chemistry **35**, 209(1997).
7. S. Cradock, R. H. Findlay and M. H. Palmer, Tetrahedron, **29**, 2173 (1973).
8. M. H. Palmer, I. Simpson and J. R. Wheeler, Z. Naturforsch., 3**6A**,1246 (1981).
9. M. H. Palmer and A. J. Beveridge, Chemical Physics **111,** 249(1987).
10. M. H. Palmer, T. Ridley, S. Vrønning Hoffmann, N. C. Jones, M. Coreno, M. de Simone, C, Grazioli, Teng Zhang, M, Biczysko, A, Baiardi, and K, A. Peterson, J. Chem. Phys. **142**, 134301 (2015).
11. M.H. Palmer, M. Biczysko, A. Baiardi, M. Coreno, M. de Simone, C.Grazioli, , S. Vrønning Hoffmann, N. C. Jones and K. A. Peterson. J. Chem. Phys., **147**, 074305 (2017)
12. M. J. Frisch, G. W. Trucks, H. B. Schlegel, G. E. Scuseria, M. A. Robb, J. R. Cheeseman, G. Scalmani, V. Barone, B. Mennucci, G. A. Petersson, H. Nakatsuji, M. Caricato, X. Li, H. P. Hratchian,A. F. Izmaylov, J. Bloino, G. Zheng, J. L. Sonnenberg, M. Hada, M. Ehara, K. Toyota, R. Fukuda, J. Hasegawa, M. Ishida, T. Nakajima, Y. Honda, O. Kitao, H. Nakai, T. Vreven, J. A. Montgomery, Jr., J. E. Peralta, F. Ogliaro, M. Bearpark, J. J. Heyd, E. Brothers, K. N. Kudin, V. N. Staroverov, T. Keith, R. Kobayashi, J. Normand, K. Raghavachari, A. Rendell, J. C. Burant, S. S. Iyengar, J. Tomasi, M. Cossi, N. Rega, J. M. Millam, M. Klene, J. E. Knox, J. B. Cross, V. Bakken, C. Adamo, J. Jaramillo, R. Gomperts, R. E. Stratmann, O. Yazyev, A. J. Austin, R. Cammi, C. Pomelli, J. W. Ochterski, R. L. Martin, K. Morokuma, V. G. Zakrzewski, G. A. Voth, P. Salvador, J. J. Dannenberg, S. Dapprich, A. D. Daniels, O. Farkas, J. B. Foresman, J. V. Ortiz, J. Cioslowski, and D. J. Fox, Gaussian 09, Revision D.01, Gaussian, Inc., Wallingford CT, 2013.

13. M. F. Guest, I. J. Bush, H. J. J. Van Dam, P. Sherwood, J. M. H. Thomas, J. H. Van Lenthe, R. W. A. Havenith, and J. Kendrick, Mol. Phys. **103**, 719 (2005).
14. V. R. Saunders and I. H Hillier, Int. J. Quantum Chemistry **7**, 699 (2004).
15. M. F. Guest and V. R. Saunders, Molec. Phys., **28**, 819-828 (1974
16. J. F. Stanton and R. J. Bartlett, J. Chem. Phys., **98** 7029 (1993).
17. J. F. Stanton and J. Gauss, J. Chem. Phys. **101**, 8938 (1994).
18. M. Kállay and J. Gauss, J. Chem. Phys., **121,** 9257 (2004).
19. CFOUR, Coupled-Cluster techniques for Computational Chemistry, a quantum-chemical program package by J. F. Stanton, J. Gauss, M. E. Harding, P. G. Szalay with contributions from A. A. Auer, R. J. Bartlett, U. Benedikt, C. Berger, D. E. Bernholdt, Y. J. Bomble, L. Cheng, O. Christiansen, M. Heckert, O. Heun, C. Huber, T.-C. Jagau, D. Jonsson, J. Juselius,K. Klein, W. J. Lauderdale, F. Lipparini, D. A. Matthews, T. Metzroth, L. A. Muck, D. P. O'Neill, D. R. Price, E. Prochnow, C. Puzzarini, K. Ruud, F. Schiffmann, W. Schwalbach, C. Simmons, S. Stopkowicz, A. Tajti, J. Vazquez, F. Wang, J. D. Watts, and the integral packages MOLECULE (J. Almlof and P. R. Taylor), PROPS (P. R. Taylor), ABACUS (T. Helgaker, H. J. A. Jensen, P. Jorgensen, and J. Olsen), and ECP routines by A. V. Mitin and C. van Wullen. For the current version, 2010, see http://www.cfour.de.
20. H.-J. Werner, P. J. Knowles, F. R. Manby, M. Schütz, P. Celani, T. Korona, R. Lindh, A. Mitrushenkov, G. Rauhut, K. R. Shamasundar, T. B. Adler, R. D. Amos, A. bernhardsson, A. berning, D. L. Cooper, M. J. O. Deegan, A. J. Dobbyn, F. Eckert, E. Goll, C. Hampel, A. Hesselmann, G. Hetzer, T. Hrenar, G. Jansen, C. Köppl,Y. Liu, A.W. Lloyd, R. A. Mata, A. J. May, S. J. McNicholas, W. Meyer, M. E. Mura, A. Nicklaß, D.P. O'Neill, P. Palmieri, K. Pflüger, R. Pitzer, M. Reiher, T. Shiozaki, H. Stoll, A. J. Stone, R. Tarroni, T. Thorsteinsson, M.Wang, and A.Wolf, MOLPRO, Version 2015.1.11, 'A package of ab initio programs, 2015,' see http://www.molpro.net.
21. R. J. Buenker and S. Krebs, in 'Recent Advances in Multireference Methods', edited by K. Hirao (World Scientific, Singapore, 1999), pp. 1–29.
22. R. A. Kendall, T. H. Dunning and R. J. Harrison, J. Chem. Phys. **96**, 6796 (1992); T. H. Dunning, J. Chem. Phys., **90** 1007-23 (1989).
23. D. Rappoport and F. Furche, J. Chem. Phys. **133**, 134105 (2010).
24. F. Weigend and A. Baldes, J. Chem. Phys. **133**, 174102 (2010).
25. V. Barone, J. Bloino, and M. Biczysko, Vibrationally-resolved electronic spectra in GAUSSIAN 09 Revision A.02 (2009) http://dreamslab.sns.it, accessed April 01, 2016.
26. J. Bloino, M. Biczysko, O. Crescenzi, and V. Barone, J. Chem. Phys. **128**, 244105 (2008).
27. V. Barone, J. Bloino, M. Biczysko, and F. Santoro, J. Chem. Theory Comput. **5**, 540 (2009).
28. J. Bloino, M. Biczysko, F. Santoro, and V. Barone, J. Chem. Theory Comput. **6**, 1256 (2010).
29. V. Barone, M. Biczysko, J. Bloino, Phys. Chem. Chem. Phys., **16**, 1759 (2014).
30. M. H. Palmer and S. Parsons, Acta Cryst., **52C**, 2818 (1996).
31. M. H. Palmer, R. H. Findlay and A. J. Gaskell, J. Chem. Soc. Perkin II, 420 (1974).
32. H. H. Jaffé and M. Orchin, 'Theory and Applications of Ultraviolet Spectroscopy,' John Wiley, New York, Chapters 12, p244 and 14, p347 et seq (1963).

33. G. Herzberg, 'Molecular Spectra and Molecular Structure' III. Electronic Spectra and Electronic Structure of Polyatomic Molecules, Van Nostrand Reinhold, New York, Chapter III, p.328, p.397 (1966).
34. L. S. Cederbaum and W. Domcke, Adv. Chem. Phys., **36**, 205 (1977).
35. J. Schirmer and L. S. Cederbaum, J. Phys., **B11**, 1889 (1978).
36. L. S. Cederbaum, W. Domcke, J. Schirmer and H. Koppel, J. Chem. Phys., **72**, 1348 (1980).
37. D. W. Turner, C. Baker, A. D. Baker and C. R. Brundle, 'Molecular Photoelectron Spectroscopy', Wiley-Interscience, London, Chapter 12, Sections 2 and 3, p324-329 (1970).
38. E. Heilbronner, J. P. Maier and E. Haselbach, 'Physical Methods in Heterocyclic Chemistry', Ed. A. R. Katritzky, Academic Press, Chapter 1, p. 1-52 (1974).

Table I. Comparison of observed with theoretical values of AIE and VIE (eV). The MRD-CI and EOM-IP-CCSD columns of VIE show a close relationship, with adjacent R^2 correlation coefficient 0.993; the slope of 0.839 is an indication of the higher level of configuration interaction in the MRD-CI results.

Exptl. PES		**State**	**UHF MP2**	**EOM-IP-CCSD**	**EOM-IP-CCSD**	**MRD-CI**
1-Methyl-tetrazole						
AIE/eV	**VIE/eV**		**AIE/eV**	**AIE/eV**	**VIE/eV**	**VIE/ eV**
10.315(1)	10.478(1)	$1^2A'$	10.563	10.275	10.742	10.136
	11.432(2)	$2^2A'$	10.645		11.084	10.606
	and	$1^2A''$	11.545	10.540	11.111	10.611
	11.846(2)	$2^2A''$	11.898		11.148	10.817
12.792(1)	12.957(2)	$3^2A'$	-		13.168	12.239
		$3^2A''$	-		15.424	14.250
2-Methyl-tetrazole						
10.543(1)	10.800(1)	$1^2A''$	10.500	10.253	10.471	10.338
	11.532	$1^2A'$	10.747	10.475	10.918	10.412
	and	$2^2A''$			11.494	11.015
	11.591(2)	$2^2A'$			11.602	11.091
13.195(1)	13.195(1)	$3^2A'$			13.463	13.049
		$3^2A''$			15.240	13.481

Table II. Harmonic (Harm) and anharmonic (Anharm) frequencies (cm^{-1}) for the X^1A' ground states and first ionic state of each symmetry for *1-* and *2-MeTet.* The calculations are at the MP2 level using the aug-cc-pVTZ basis set.

State	*1-MeTet*				*2-MeTet*			
	X^1A'		$2A'$	$2A''$	X^1A'		$2A'$	$2A''$
Mode	Anharm.	Harm.	Harm.	Harm.	Anharm.	Harm.	Harm. 89550.1885	Harm. 90950.9572
1a/	3335	3429	3316	3277	3345	3448	3334	3296
2a/	3142	3286	3228	3235	3205	3325	3243	3234
3a/	3025	3202	3107	3108	3146	3217	3108	3070
4a/	1650	1687	1731	2825	1653	1682	1751	2778
5a/	1611	1655	1570	1555	1589	1628	1569	1648
6a/	1574	1609	1492	1507	1555	1584	1489	1480
7a/	1552	1585	1464	1444	1546	1572	1463	1432
8a/	1500	1526	1423	1327	1437	1471	1367	1356
9a/	1379	1413	1360	1245	1424	1453	1294	1284
10a/	1311	1332	1204	1181	1367	1394	1243	1204
11a/	1224	1246	1190	1129	1228	1255	1112	1153
12a/	1136	1157	1106	1098	1138	1158	1097	1046
13a/	1111	1137	1057	1001	1122	1143	1021	984
14a/	1078	1097	875	899	1112	1130	957	734
15a/	732	742	662	663	754	766	683	656
16a/	381	381	358	349	403	406	371	361
17a//	3171	3277	3231	3222	3183	3292	3224	3163
18a//	1559	1599	1483	1502	1562	1601	1485	1469
19a//	1237	1256	1163	1171	1238	1256	1149	1118
20a//	995	1013	858	957	999	1009	961	983
21a//	806	816	682	552	786	793	757	683
22a//	718	728	443	435	750	760	290	542
23a//	233	238	281	254	245	252	102	263
24a//	59	68	71	33	77	84	-236	-97

Table III. The principal components contributing to the intensity (molar absorption coefficient /dm^3.mol^{-1}.cm^{-1}) of the 1-MeTet PES onset. The vibration frequency (cm^{-1}) calculations were performed with the aug-cc-pVTZ basis set at the MP2 level, and are unscaled. Numerous additional combination and overtones, making weaker contributions, which are mainly responsible for the line broadening are given in the supplementary information as SM4.

X^2A' state of *1-MeTet*			**A^2A'' state of *1-MeTet***		
Wavenumber / cm^{-1}	Assignment	Intensity	Wavenumber / cm^{-1}	Assignment	Intensity
0	0^0	12900	0	0^0	452500
875	14^1	5437	663	15^1	128400
1057	13^1	3134	871	22^2	8594
1106	12^1	8163	899	14^1	79510
1204	10^1	4198	1001	13^1	37370
1423	8^1	25639	1098	12^1	258700
1565	8^124^2	2274	1104	21^2	2067
1731	4^1	13687	1129	11^1	40610
1981	12^114^1	3484	1181	10^1	13720
2213	12^2	2580	1245	9^1	30210
2298	8^214^1	10947	1326	15^2	24380
2479	8^113^1	6370	1327	8^1	71970
2529	8^112^1	15830	1444	7^1	11540
2606	4^114^1	5801	1555	5^1	6936
2845	8^2	27869	1990	15^3	2558
2988	8^224^2	2463	2195	12^2	67520
3462	4^2	9722	2257	11^2	2232
3720	8^114^1	12011	2490	9^2	2461
4268	8^3	21762	2654	8^2	7348
5193	4^3	5583	2825	4^1	24440
5691	8^4	13643	3293	12^3	10670
6923	4^4	2784	5649	4^2	43080
7113	8^5	7273	8474	4^3	5787
8536	8^6	3411	11299	4^4	5842

Table IV. The principal components contributing to the intensity (molar absorption coefficient /dm^3.mol^{-1}.cm^{-1}) of the 2-MeTet PES onset. The vibration frequency (cm^{-1}) calculations were performed with the aug-cc-pVTZ basis set at the MP2 level, and are unscaled. Numerous additional combination and overtones making weaker contributions, which are mainly responsible for the line broadening are given in the supplementary information.

^{2}A$^{/}$ state of *2-MeTet*			**^{2}A$^{//}$ state of *2-MeTet***		
Wavenumber / cm^{-1}	Assignment	Intensity	Wavenumber / cm^{-1}	Assignment	Intensity
0	0^0	34550	0	0^0	24260
957	14^1	64620	360.9762	16^1	1233
1097	12^1	28470	656.4822	15^1	9109
1243	10^1	15950	734.0230	14^1	9243
1294	9^1	4097	983.7405	13^1	6432
1463	7^1	1160	1045.7967	12^1	9259
1569	5^1	6453	1084.3285	22^2	242
1751	4^1	4059	1152.9250	11^1	4904
1915	14^2	82860	1283.8940	9^1	4383
2054	$12^1 14^1$	51970	1312.9644	15^2	739
2069	$11^1 14^1$	1519	1344.7167	$13^1 16^1$	326
2193	12^2	11280	1390.5052	$14^1 15^1$	1799
2200	$10^1 14^1$	39930	1406.7729	$\|12^1 16^1$	530
2251	$13^1 14^1$	11650	1468.0460	14^2	
2339	$10^1 12^1$	12620	1513.9012	$11^1 16^1$	841
2420	$7^1 14^1$	3220	1640.2227	$13^1 15^1$	248
2447	$6^1 14^1$	2488	1644.8702	$9^1 16^1$	2345
2527	$5^1 14^1$	11210	1702.2789	$12^1 15^1$	166
2709	$4^1 14^1$	12110	1717.7635	$13^1 14^1$	3033
2486	10^2	1301	1779.8197	$12^1 14^1$	2625
2872	14^3	62190	1809.4072	$11^1 15^1$	3643
3012	$12^1 14^2$	70570	1860.3614	$\|10^1 15^1$	1577
3209	$9^1 14^2$	14570	1886.9480	$11^1 14^1$	254
3290	12^3	2858	1937.9023	$10^1 14^1$	1633
3502	4^2	1313	1940.3761	$9^1 15^1$	414
3830	14^4	25170	1967.4810	13^2	1385
4787	14^5	11510	2091.5934	12^2	761
5745	14^6	3818	2305.8501	11^2	1424
3151	$12^2 14^1$	20090			

Figure Captions

Fig. 1. Tautomerism occurs in the tetrazole system 1 and 2 for R = H. Interconversion is blocked by N-methylation (R = Me) enabling to two distinct ring systems to be studied.

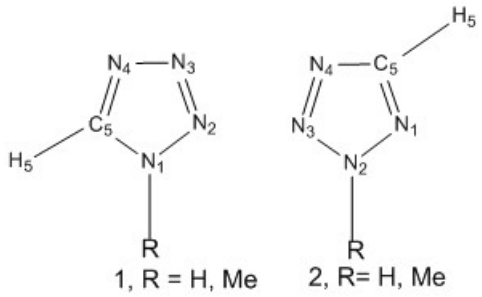

Fig. 2. The classical structures of the 1- and 2-methyl-tetrazoles, where the 'lone pair electrons' are indicated. The internal rotation of the methyl groups takes place in an unsymmetrical ring structure, leading to distinct conformers, with a repeating pattern after 120º. The methyl group H-atoms at the C_s conformation are marked 'ip' for in-plane, 'oop' for out-of-plane. For both the 1- and 2-methyl compounds, the $H_{ip}CN_2N_3$ dihedral angles with minimum energies are 60, 180 and 300º. For 2-methyl, two minima differing by 180 cm^{-1} occur with the lowest energy conformer being shown. For the 1-methyl conformer, the 180º conformer has lowest energy by 11.2 cm^{-1}, with the barrier (120ºand 0º) higher by 92 cm^{-1}.

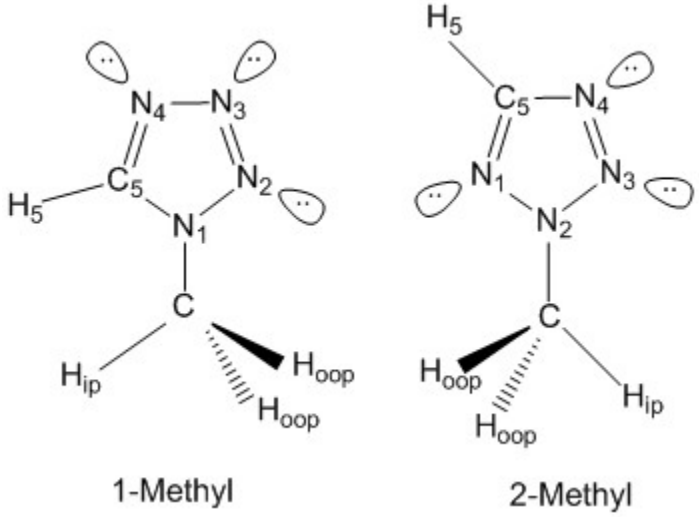

Fig.3. Comparison of the PES spectra for the 1- and 2-methyl-tetrazoles with colours blue and red respectively. The difference in count rates reflects the relative vapor pressures. All of the present calculations show that the 10 to 14 eV range of the PES spectra contain 5 IE for each isomer, in the ratio 4 to 1. The groups of 4 consist of two π-ionizations (π^{-1}, $^2A''$) and two lone-pair ionizations (LP_N^{-1}, $^2A'$) as indicated. The theoretical AIE shown in black are unrestricted Hartree-Fock (UHF) calculations.

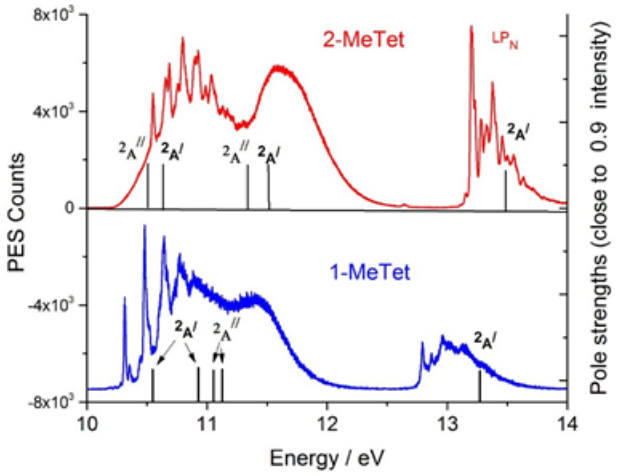

Fig. 4. The four highest lying MOs of 1-MeTet. MOs 22 and 21 are the π4- and π3-orbitals. MOs 20 and 19 are the two highest LP_N MOs, $1^2A'$ and $2^2A'$. These are largely linear combinations of $LP_{N2} - LP_{N4}$ and LP_{N3} respectively. The corresponding MOs for 2-MeTet are of similar style.

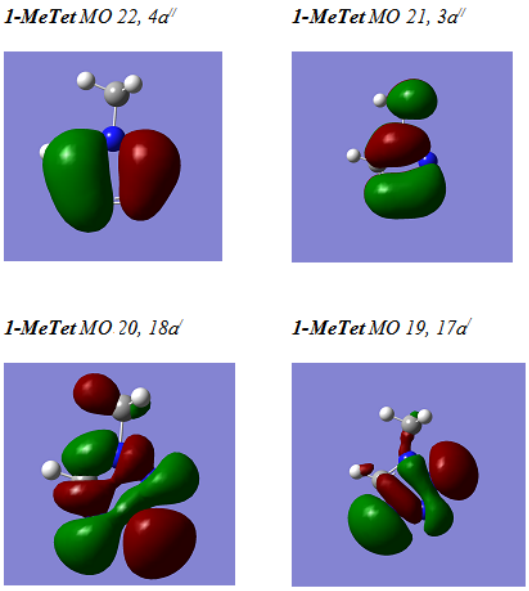

Fig. 5. The onset of ionization for 1-MeTet. The Franck-Condon vibrational profile has been super-imposed using a FWHM 75 cm^{-1} (red) and 100 cm^{-1} (blue); the theoretical harmonic values have been scaled by 0.98 to improve the correlation, a value in the normal range. The 'stick' diagram in magenta shows the complexity of the peaks. Almost all the observed detail below 85836 cm^{-1} is reproduced by the X^2A' state alone. This value is assigned to the 0-0 band of the more intense A^2A'' state as indicated, and shown in Figure 6. The two wave-trains overlap significantly, leading to destructive interference in a vibronic coupling effect, witnessed on the higher energy ionic state.

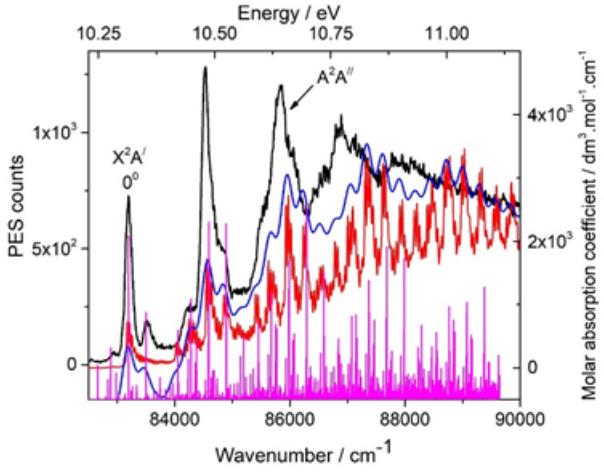

Fig. 6. The second ionization for 1-MeTet with the Franck-Condon vibrational profile super-imposed with FWHM 10 (red) and 150 cm^{-1} (blue). The very much larger FWHM value is necessary to generate a profile similar to experiment shows the effect of the destructive interference on the A^2A'' state vibrational waveform by the lower X^2A' state interference.

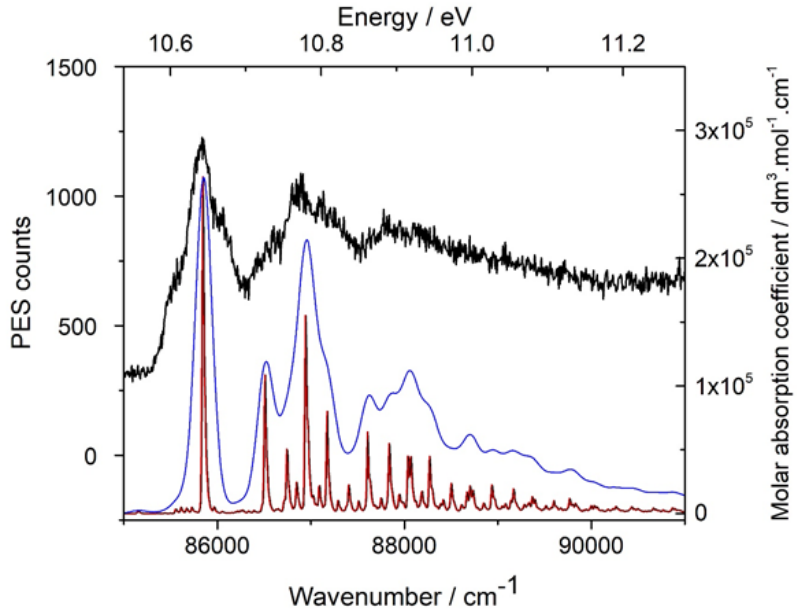

Fig. 7. The onset of the photoelectron spectrum of 2-MeTet. The Franck-Condon diagram profiles for the two lowest ionizations have been widened to 100 cm^{-1} in order to indicate the much larger effect necessary to account for the unusual very slow onset. The $1^2A'$ state has a very low 0-0 band intensity, in contrast to that for the $1^2A''$ state. There is accidental degeneracy of one vibration of the X^2A' state with the 0-0 band of the A^2A'' state at 85060 cm^{-1} (10.546 eV).

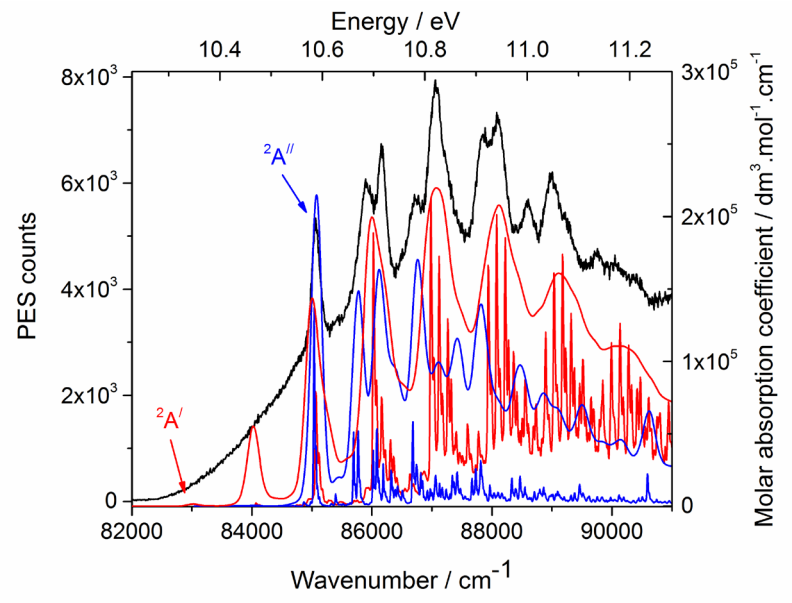

Fig. 8. A portion of the VUV spectrum (in black) of 2-MeTet. Two Rydberg state assignments (red and blue) are made by double super-position of the PES spectrum. This overlay shows that not all of the peaks in the PES relate to one IE.